

# Nitrous oxide emission from denitrification in stream and river networks

Jake J. Beaulieu<sup>a,1,2</sup>, Jennifer L. Tank<sup>a</sup>, Stephen K. Hamilton<sup>b</sup>, Wilfred M. Wollheim<sup>c</sup>, Robert O. Hall, Jr.<sup>d</sup>, Patrick J. Mulholland<sup>e,f</sup>, Bruce J. Peterson<sup>g</sup>, Linda R. Ashkenas<sup>h</sup>, Lee W. Cooper<sup>i</sup>, Clifford N. Dahm<sup>j</sup>, Walter K. Dodds<sup>k</sup>, Nancy B. Grimm<sup>l</sup>, Sherri L. Johnson<sup>m</sup>, William H. McDowell<sup>n</sup>, Geoffrey C. Poole<sup>o</sup>, H. Maurice Valett<sup>p</sup>, Clay P. Arango<sup>q</sup>, Melody J. Bernot<sup>r</sup>, Amy J. Burgin<sup>s</sup>, Chelsea L. Crenshaw<sup>j</sup>, Ashley M. Helton<sup>t</sup>, Laura T. Johnson<sup>u</sup>, Jonathan M. O'Brien<sup>v</sup>, Jody D. Potter<sup>n</sup>, Richard W. Sheibley<sup>l,3</sup>, Daniel J. Sobota<sup>w</sup>, and Suzanne M. Thomas<sup>g</sup>

<sup>a</sup>Department of Biological Sciences, University of Notre Dame, Notre Dame, IN 46556; <sup>b</sup>Kellogg Biological Station, Michigan State University, Hickory Corners, MI 49060; <sup>c</sup>Department of Natural Resources and Environment and Complex Systems Research Center, Institute for the Study of Earth, Oceans, and Space, University of New Hampshire, Durham, NH 03824; <sup>d</sup>Department of Zoology and Physiology, University of Wyoming, Laramie, WY 82071; <sup>e</sup>Environmental Sciences Division, Oak Ridge National Laboratory, Oak Ridge, TN 37831; <sup>f</sup>Department of Ecology and Evolutionary Biology, University of Tennessee, Knoxville, TN 37996; <sup>g</sup>Ecosystems Center, Marine Biological Laboratory, Woods Hole, MA 02543; <sup>h</sup>Department of Fisheries and Wildlife, Oregon State University, Corvallis, OR 97331; <sup>i</sup>Chesapeake Biological Laboratory, University of Maryland Center for Environmental Science, Solomons, MD, 20688; <sup>j</sup>Department of Biology, University of New Mexico, Albuquerque, NM 87131; <sup>k</sup>Division of Biology, Kansas State University, Manhattan, KS 66506; <sup>l</sup>School of Life Sciences, Arizona State University, Tempe, AZ 85287; <sup>m</sup>Pacific Northwest Research Station, US Forest Service, Corvallis, OR 97331; <sup>n</sup>Department of Natural Resources and the Environment, University of New Hampshire, Durham, NH 03824; <sup>o</sup>Department of Land Resources and Environmental Sciences, Montana State University, Bozeman, MT 59717; <sup>p</sup>Department of Biological Sciences, Virginia Polytechnic Institute and State University, Blacksburg, VA 24061; <sup>q</sup>Department of Biological Sciences, Central Washington University, Ellensburg, WA 98926; <sup>r</sup>Department of Biology, Ball State University, Muncie, IN 47306; <sup>s</sup>Department of Earth and Environmental Sciences, Wright State University, Dayton, OH 45435; <sup>t</sup>Odum School of Ecology, University of Georgia, Athens, GA 30602; <sup>u</sup>School of Public and Environmental Affairs, Indiana University, Bloomington, IN 47405; <sup>v</sup>School of Biological Sciences, University of Canterbury, Christchurch 8014, New Zealand; and <sup>w</sup>School of Earth and Environmental Sciences, Washington State University, Vancouver, WA 98686

Edited\* by William H. Schlesinger, Cary Institute of Ecosystem Studies, Millbrook, NY, and approved November 11, 2010 (received for review August 4, 2010)

**Nitrous oxide (N<sub>2</sub>O) is a potent greenhouse gas that contributes to climate change and stratospheric ozone destruction. Anthropogenic nitrogen (N) loading to river networks is a potentially important source of N<sub>2</sub>O via microbial denitrification that converts N to N<sub>2</sub>O and dinitrogen (N<sub>2</sub>). The fraction of denitrified N that escapes as N<sub>2</sub>O rather than N<sub>2</sub> (i.e., the N<sub>2</sub>O yield) is an important determinant of how much N<sub>2</sub>O is produced by river networks, but little is known about the N<sub>2</sub>O yield in flowing waters. Here, we present the results of whole-stream <sup>15</sup>N-tracer additions conducted in 72 headwater streams draining multiple land-use types across the United States. We found that stream denitrification produces N<sub>2</sub>O at rates that increase with stream water nitrate (NO<sub>3</sub><sup>-</sup>) concentrations, but that <1% of denitrified N is converted to N<sub>2</sub>O. Unlike some previous studies, we found no relationship between the N<sub>2</sub>O yield and stream water NO<sub>3</sub><sup>-</sup>. We suggest that increased stream NO<sub>3</sub><sup>-</sup> loading stimulates denitrification and concomitant N<sub>2</sub>O production, but does not increase the N<sub>2</sub>O yield. In our study, most streams were sources of N<sub>2</sub>O to the atmosphere and the highest emission rates were observed in streams draining urban basins. Using a global river network model, we estimate that microbial N transformations (e.g., denitrification and nitrification) convert at least 0.68 Tg·y<sup>-1</sup> of anthropogenic N inputs to N<sub>2</sub>O in river networks, equivalent to 10% of the global anthropogenic N<sub>2</sub>O emission rate. This estimate of stream and river N<sub>2</sub>O emissions is three times greater than estimated by the Intergovernmental Panel on Climate Change.**

Humans have more than doubled the availability of fixed nitrogen (N) in the biosphere, particularly through the production of N fertilizers and the cultivation of N-fixing crops (1). Increasing N availability is producing unintended environmental consequences including enhanced emissions of nitrous oxide (N<sub>2</sub>O), a potent greenhouse gas (2) and an important cause of stratospheric ozone destruction (3). The Intergovernmental Panel on Climate Change (IPCC) estimates that the microbial conversion of agriculturally derived N to N<sub>2</sub>O in soils and aquatic ecosystems is the largest source of anthropogenic N<sub>2</sub>O to the atmosphere (2). The production of N<sub>2</sub>O in agricultural soils has been the focus of intense investigation (i.e., >1,000 published studies) and is a relatively well constrained component of the N<sub>2</sub>O budget (4). However, emissions of anthropogenic N<sub>2</sub>O from streams, rivers, and estuaries have received much less attention

and remain a major source of uncertainty in the global anthropogenic N<sub>2</sub>O budget.

Microbial denitrification is a large source of N<sub>2</sub>O emissions in terrestrial and aquatic ecosystems. Most microbial denitrification is a form of anaerobic respiration in which nitrate (NO<sub>3</sub><sup>-</sup>, the dominant form of inorganic N) is converted to dinitrogen (N<sub>2</sub>) and N<sub>2</sub>O gases (5). The proportion of denitrified NO<sub>3</sub><sup>-</sup> that is converted to N<sub>2</sub>O rather than N<sub>2</sub> (hereafter referred to as the N<sub>2</sub>O yield and expressed as the mole ratio) partially controls how much N<sub>2</sub>O is produced via denitrification (6), but few studies provide information on the N<sub>2</sub>O yield in streams and rivers because of the difficulty of measuring N<sub>2</sub> and N<sub>2</sub>O production in these systems. Here we report rates of N<sub>2</sub> and N<sub>2</sub>O production via denitrification measured using whole-stream <sup>15</sup>NO<sub>3</sub><sup>-</sup>-tracer experiments in 72 headwater streams draining different land-use types across the United States. This project, known as the second Lotic Intersite Nitrogen eXperiment (LINX II), provides unique whole-system measurements of the N<sub>2</sub>O yield in streams.

Although N<sub>2</sub>O emission rates have been reported for streams and rivers (7, 8), the N<sub>2</sub>O yield has been studied mostly in lentic freshwater and marine ecosystems, where it generally ranges between 0.1 and 1.0%, although yields as high as 6% have been observed (9). These N<sub>2</sub>O yields are low compared with observations in soils (0–100%) (10), which may be a result of the relatively lower oxygen (O<sub>2</sub>) availability in the sediments of lakes and estuaries. However, dissolved O<sub>2</sub> in headwater streams is commonly near atmospheric equilibrium and benthic algal bio-

Author contributions: J.L.T., S.K.H., R.O.H., P.J.M., B.J.P., L.R.A., L.W.C., C.N.D., W.K.D., N.B.G., S.L.J., W.H.M., G.C.P., and H.M.V. designed research; J.J.B., J.L.T., S.K.H., W.M.W., R.O.H., P.J.M., B.J.P., L.R.A., W.K.D., N.B.G., S.L.J., W.H.M., H.M.V., C.P.A., M.J.B., A.B., C.C., A.M.H., L.T.J., J.M.O., J.D.P., R.W.S., D.J.S., and S.M.T. performed research; J.J.B. analyzed data; J.J.B., J.L.T., and S.K.H. wrote the paper; and W.M.W. performed the global river N<sub>2</sub>O production modeling.

The authors declare no conflict of interest.

\*This Direct Submission article had a prearranged editor.

Freely available online through the PNAS open access option.

<sup>1</sup>Present address: US Environmental Protection Agency, Cincinnati, OH 45268.

<sup>2</sup>To whom correspondence should be addressed. E-mail: beaulieu.jake@epa.gov.

<sup>3</sup>Present address: US Geological Survey Water Science Center, Tacoma, WA 98402.

This article contains supporting information online at [www.pnas.org/lookup/suppl/doi:10.1073/pnas.1011464108/-DCSupplemental](http://www.pnas.org/lookup/suppl/doi:10.1073/pnas.1011464108/-DCSupplemental).

films can produce  $O_2$  at the sediment–water interface, resulting in strong redox gradients more akin to those in partially wetted soils. Thus, streams may have variable and often high  $N_2O$  yields, similar to those in soils (11). The  $N_2O$  yield in headwater streams is of particular interest because much of the  $NO_3^-$  input to rivers is derived from groundwater upwelling into headwater streams. Furthermore, headwater streams compose the majority of stream length within a drainage network and have high ratios of bio-reactive benthic surface area to water volume (12).

## Results and Discussion

The  $^{15}N$ - $NO_3^-$  tracer was detected in the dissolved  $N_2O$  pool in 53 of 72 streams and we assume that direct denitrification of stream water  $NO_3^-$  to  $N_2O$  ( $N_2O_{DN}$ ) was the source of this  $^{15}N$ - $N_2O$ . It is unlikely that nitrification was an important source of labeled  $^{15}N$ - $N_2O$  because the 24-h duration of the experiments was too short for the tracer to be assimilated by stream biota, mineralized, and subsequently nitrified. Rates of  $N_2O_{DN}$  varied by land use with the highest rates observed in high  $NO_3^-$  urban streams and the lowest in reference streams (i.e., those with little land conversion in their watersheds) (Fig. 1A). A positive relationship between  $N_2O_{DN}$  and stream water  $NO_3^-$  concentration (Fig. 1B) suggests anthropogenic N loading to streams stimulates

denitrification and concomitant  $N_2O$  production. The  $N_2O_{DN}$  rates reported here are lower than most published reports (Fig. 1A), possibly because our in situ measurements are not affected by the experimental artifacts and scaling problems associated with sediment slurries, cores, and chambers used in most previously published estimates (13).

The  $^{15}N$ - $NO_3^-$  tracer was detected in both the dissolved  $N_2$  and  $N_2O$  pools in 40 of the 72 study sites and we assume all  $^{15}N$ - $N_2$  was produced via direct denitrification. The only other potential source of  $^{15}N$ - $N_2$  production is anammox, a process by which chemolithoautotrophic bacteria convert ammonium ( $NH_4^+$ ) and nitrite ( $NO_2^-$ ) to  $N_2$ , but available evidence suggests that anammox is unimportant relative to denitrification in streams and rivers (14). Furthermore, any  $N_2$  produced via anammox during the  $^{15}N$  tracer additions would have contained little  $^{15}N$  tracer because stream water  $NH_4^+$  was minimally labeled with the  $^{15}N$  tracer.

The  $N_2O$  yield ranged from 0.04% to 5.6% across the 53 streams; however, the interquartile range (0.3–1.0%) was well constrained despite substantial variation in  $NO_3^-$  availability, dissolved  $O_2$ , primary productivity, sediment organic matter, and stream geomorphology across our study sites (Fig. 2, Table S1). Denitrification proceeds by sequentially reducing  $NO_3^-$  to  $NO_2^-$ , nitric oxide (NO),  $N_2O$ , and finally  $N_2$ . Each reduction is per-

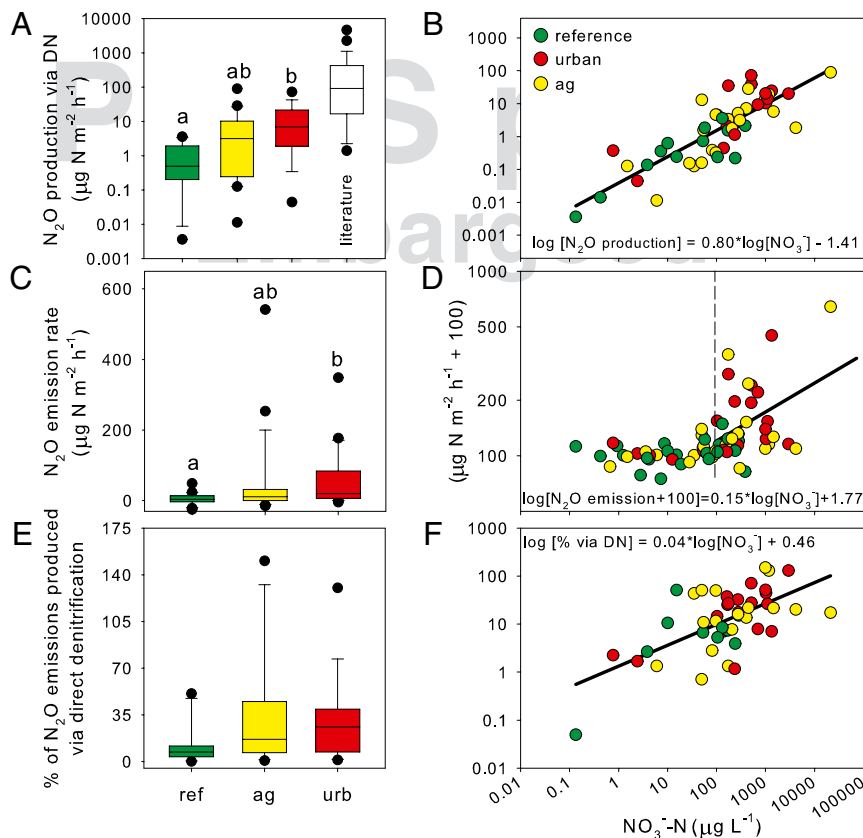


**Fig. 1.** (A) Box plots of stream  $N_2O$  production rates via denitrification of water column  $NO_3^-$  by catchment land use (reference, agricultural and urban). Benthic  $N_2O$  production rates reported in other studies are also shown. Significant differences between land-use types were determined with a one-way ANOVA followed by Tukey's post hoc test ( $P = 0.004$ ) and are displayed as different lowercase letters above the box plots. See *SI Materials and Methods* for references. (B) Relationship between stream water  $NO_3^-$  and rates of  $N_2O$  production via denitrification ( $r^2 = 0.68$ ,  $P < 0.001$ ). (C) Nitrous oxide emission rates from streams. Significant differences between land use types were determined with a one-way ANOVA ( $P = 0.002$ ) followed by Tukey's post hoc test and are displayed as different lowercase letters above the box plots. (D) Relationship between stream water  $NO_3^-$  concentrations and  $N_2O$  emission rates. The vertical dashed line represents a  $NO_3^-$  threshold ( $95 \mu g N L^{-1}$ ) below which  $N_2O$  emission rates are unrelated to  $NO_3^-$  (two-dimensional Kolmogorov–Smirnov test). Above the threshold  $N_2O$  emission rates are positively related to  $NO_3^-$  concentrations as represented by the least-squares best-fit line (solid black). (E) Percentages of stream  $N_2O$  emissions attributed to direct denitrification. Values  $>100\%$  indicate  $N_2O$  was accumulating in the water column. There was no effect of land use ( $P = 0.13$ ). (F) Variation in the percentage of stream  $N_2O$  emissions attributed to direct denitrification is partially explained by stream water  $NO_3^-$  concentration ( $r^2 = 0.32$ ,  $P < 0.001$ ).

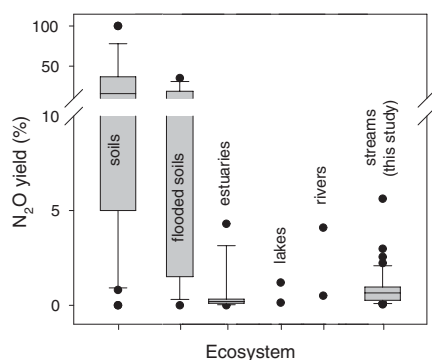


**Fig. 2.** Denitrification  $N_2O$  yields (percentage of denitrified N released as  $N_2O$ ) measured in this study in comparison with other ecosystems. Data are displayed in box plots unless there were fewer than nine observations, in which case each observation is represented by a solid circle. See *SI Materials and Methods* for references.

formed by a different enzyme and the  $N_2O$  yield is determined by the relative activities of the  $N_2O$ -producing and reducing enzymes. There is a positive relationship between the  $N_2O$  yield and  $NO_3^-$  concentration in soils (15, 16) and estuarine sediments (9), possibly because higher  $NO_3^-$  availability suppresses nitrous oxide reductase (*nos*), the enzyme that reduces  $N_2O$  to  $N_2$  (16). However, we did not find a significant relationship between stream water  $NO_3^-$  concentration and the  $N_2O$  yield ( $P = 0.09$ ), despite  $NO_3^-$  concentrations spanning five orders of magnitude. Our findings suggest increased  $NO_3^-$  loading to streams stimulates overall denitrification rates and concomitant  $N_2O$  production, but does not increase the  $N_2O$  yield.

The  $N_2O$  yield in soils is related to the relative availability of oxidants ( $NO_3^-$ ) and reductants (organic carbon). When the availability of  $NO_3^-$  greatly exceeds that of organic carbon,  $NO_3^-$  is preferred over  $N_2O$  as a terminal electron acceptor and  $N_2O$  accumulates (5, 17–19). The  $N_2O$  yield was not related to the ratio of stream water  $NO_3^-$  concentration to dissolved or particulate organic carbon concentration ( $P \geq 0.17$ ), but was negatively related to stream ecosystem respiration ( $P = 0.04$ ,  $r^2 = 0.11$ ), suggesting factors promoting aerobic respiration (e.g., labile carbon availability) may decrease the  $N_2O$  yield.

Our data suggest that denitrification in aquatic ecosystems produces lower and less variable  $N_2O$  yields than in terrestrial ecosystems (Fig. 2). This finding may be explained by differences in oxygen ( $O_2$ ) availability and molecular diffusion rates between aquatic sediments and the partially water-filled pore spaces of soils. Because *nos* is the most  $O_2$  sensitive denitrifying enzyme (20), minor amounts of  $O_2$  can suppress the reduction of  $N_2O$  without inhibiting its production, resulting in an elevated  $N_2O$  yield. Nitrous oxide is produced as a free intermediate that can escape reduction to  $N_2$  by diffusing away from the denitrification zone (16). Partially wet soils may present air-filled routes through which the  $N_2O$  could more readily evade from soil solutions and ultimately escape to the atmosphere, whereas in aquatic sediments there may be a much greater likelihood of interception of the dissolved  $N_2O$  by *nos* before it can diffuse to the overlying water column. Overall, lower  $O_2$  availability and gas diffusion rates in aquatic sediments compared with soils may account for the low aquatic  $N_2O$  yield.

Resource managers have used stream restoration to reduce watershed N export to estuaries and coastal oceans where it can contribute to eutrophication (21). This approach has been criticized on the grounds that stream denitrification alone cannot alleviate watershed N pollution (22) and that enhanced stream denitrification may lead to increased  $N_2O$  emission (23). Our data demonstrate that the  $N_2O$  yield in headwater streams is no larger

than in other aquatic ecosystems and much lower than in soils (Fig. 2), indicating that measures to promote stream denitrification may have a relatively lower impact on climate change than the promotion of an equivalent amount of denitrification in terrestrial environments.

Other sources of  $N_2O$  to streams include in-stream nitrification and upwelling groundwater. The sum of all these  $N_2O$  sources determines the total amount of  $N_2O$  emitted by a stream. We investigated the potential for these additional sources to contribute to total  $N_2O$  emissions by estimating  $N_2O$  emission rates from the dissolved  $N_2O$  concentration and the air–water gas exchange rates in each of the 72 streams. The majority of streams were net sources of  $N_2O$  to the atmosphere (55 of 72) and only 2 streams showed a diel pattern in emission rates so we did not further consider diel variations in constructing  $N_2O$  budgets (cf. ref. 24). Stream  $N_2O$  emission rates were related to watershed land use, with highest emission rates in urban streams, intermediate rates in agricultural streams, and lowest rates in reference streams (Fig. 1C). Stream  $NO_3^-$  concentrations predicted  $N_2O$  emission rates when  $NO_3^-$ -N exceeded  $95 \mu\text{g}\cdot\text{L}^{-1}$  ( $P = 0.01$ ,  $r^2 = 0.16$ ), but below this concentration  $N_2O$  emission rates were uniformly low and unrelated to  $NO_3^-$  concentration (Fig. 1D). This finding suggests that stream  $N_2O$  emission rates are not solely controlled by direct denitrification within the stream, but are likely enhanced by other sources including inputs of dissolved  $N_2O$  from groundwater.

We compared  $N_2O_{DN}$  (Fig. 14) to  $N_2O$  emission rates (Fig. 1C) and found that the direct denitrification of stream water  $NO_3^-$  accounted for an average of 26% of  $N_2O$  emissions (Fig. 1E). This is a conservative estimate of in-stream  $N_2O$  production via denitrification because our method does not detect  $N_2O$  produced from the denitrification of  $NO_3^-$  regenerated within sediments and biofilms (e.g., indirect denitrification following organic N mineralization and nitrification), which can be the dominant source of  $NO_3^-$  supporting denitrification when stream water  $NO_3^-$  concentration is low ( $<140 \mu\text{g}\cdot\text{L}^{-1}$ ) (25). The relative importance of  $N_2O_{DN}$  as a source of  $N_2O$  was positively related to stream water  $NO_3^-$  concentrations (Fig. 1F), reflecting the greater importance of direct denitrification with increasing stream water  $NO_3^-$  concentrations.

Nitrification is a potentially large source of  $N_2O$  emissions, but we know of no published measurements of  $N_2O$  production via nitrification in streams. Several studies have shown that nitrification rates can be equal to or greater than denitrification rates in streams (26–28) and rivers (29), and the IPCC assumes nitrification rates exceed denitrification by twofold (30). Measurements of the nitrification  $N_2O$  yield (i.e., the fraction of nitrified N escaping as  $N_2O$ ) are sparse, but it appears to be within the same range as the denitrification  $N_2O$  yield (9). Therefore, the IPCC assumes that nitrification produces twice as much  $N_2O$  emission as denitrification in streams and rivers. Given that  $N_2O_{DN}$  produced within the stream contributes an average of 26% of the  $N_2O$  emitted by headwater streams (Fig. 1E), nitrification could account for as much as an additional 52%, with groundwater inputs and indirect denitrification composing the remainder (Fig. 3). This budget highlights the potential importance of nitrification and indirect denitrification to stream  $N_2O$  production, but these processes remain poorly understood and therefore represent critical research gaps. Nevertheless, our research demonstrates that headwater streams are not only conduits for the emission of groundwater-derived  $N_2O$  to the atmosphere, but also active sites of in situ  $N_2O$  production, particularly where  $NO_3^-$  concentrations are elevated by anthropogenic N loading.

The IPCC and others have estimated global anthropogenic  $N_2O$  emissions from streams and rivers by assuming all anthropogenic N that enters a river network is nitrified to  $NO_3^-$  and half of this  $NO_3^-$  is then denitrified; the  $N_2O$  yield is assumed to range from 0.3% to 3.0% in each transformation (9, 30, 31). This approach has shown that streams and rivers may be the source

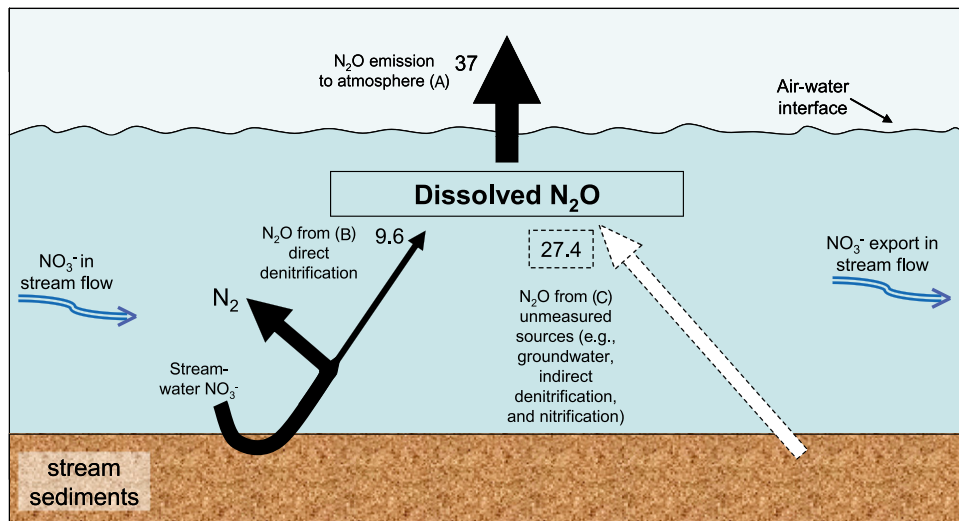


**Fig. 3.** Average  $\text{N}_2\text{O}$  fluxes estimated in this study (all units are  $\mu\text{g N}\cdot\text{m}^{-2}\cdot\text{h}^{-1}$ ). Black arrows represent fluxes that were directly measured and the white arrow with dashed boundaries represents fluxes that were estimated by mass balance. (A)  $\text{N}_2\text{O}$  produced in the stream, or imported to the stream via groundwater, temporarily resides in a pool of dissolved  $\text{N}_2\text{O}$  before being emitted to the atmosphere. (B) Direct denitrification is the conversion of stream water nitrate to  $\text{N}_2$  and  $\text{N}_2\text{O}$ . Less than 1% of stream water nitrate subject to direct denitrification is converted to  $\text{N}_2\text{O}$ , but this is the source of 26% of the  $\text{N}_2\text{O}$  emitted by the stream. (C) The balance of  $\text{N}_2\text{O}$  emission in excess of that produced via direct denitrification (e.g.,  $37 - 9.6 = 27.4$ ) must have entered the stream via another mechanism. Likely mechanisms include indirect denitrification (e.g., the denitrification of nitrate generated within the sediments), nitrification, and inputs of  $\text{N}_2\text{O}$ -supersaturated groundwater.

of 15% of global anthropogenic emissions, but this estimate is poorly constrained due to uncertainty in the  $\text{N}_2\text{O}$  yield and proportion of anthropogenic N inputs denitrified in river networks. We improved the estimate of global anthropogenic  $\text{N}_2\text{O}$  emissions from lotic systems by modifying an existing global river network model (32) to include spatially explicit N loading in the contemporary era, an empirically derived relationship between denitrification and  $\text{NO}_3^-$  concentrations based on the LINX II  $^{15}\text{N}$  tracer studies (22), and the mean  $\text{N}_2\text{O}$  yield of 0.9% reported here. The model estimates the percentage of dissolved inorganic nitrogen (DIN) delivered to the world's streams and rivers that is converted to  $\text{N}_2\text{O}$  via direct denitrification as water flows through the river network, including lakes and reservoirs. However, the model does not include indirect denitrification or denitrification associated with off-channel features (e.g., floodplains, riparian zones) and therefore provides a conservative estimate of anthropogenic  $\text{N}_2\text{O}$  emissions (Fig. 3).

The percentage of DIN inputs converted to  $\text{N}_2\text{O}$  via direct denitrification of water column  $\text{NO}_3^-$  in river networks across the globe ranges from 0% to 0.9% (Fig. 4). The percentage of N inputs converted to  $\text{N}_2\text{O}$  decreases with increasing N inputs because denitrification becomes less efficient as a  $\text{NO}_3^-$  sink at higher  $\text{NO}_3^-$  concentrations (22). We expected that the longer water-residence time in large rivers would result in a larger percentage of N inputs being denitrified compared with smaller river networks. However, we found no effect of catchment area (a surrogate for river network length), likely because the size of the network is confounded by other factors including variation in the distribution of N inputs, temperature, runoff conditions, and the presence of lakes and reservoirs within river networks (32).

We estimate that at the global scale, 0.75% of DIN inputs to river networks are converted to  $\text{N}_2\text{O}$  via direct denitrification and nitrification, threefold greater than the IPCC's estimate. This  $\text{N}_2\text{O}$  is likely to be emitted to the atmosphere from the turbulent water columns of streams and rivers. Using the IPCC's modeling framework and the results of our work, we estimate that nitrification and denitrification in river networks convert  $0.68 \text{ Tg}\cdot\text{y}^{-1}$  of anthropogenic DIN inputs to  $\text{N}_2\text{O}$  globally, equivalent to 10% of the global anthropogenic  $\text{N}_2\text{O}$  emissions of

$6.7 \text{ Tg N}\cdot\text{y}^{-1}$  (2) (for calculation details see *Global  $\text{N}_2\text{O}$  Budget in SI Materials and Methods*). This estimate of anthropogenic  $\text{N}_2\text{O}$  emissions from river networks is conservative because our model does not include several potentially large sources of  $\text{N}_2\text{O}$  (e.g., indirect denitrification and groundwater inputs). We also caution that our estimate of  $\text{N}_2\text{O}$  emissions attributed to nitrification is supported by few data (see above and Fig. 3).

We found that the combination of high denitrification rates and large anthropogenic DIN inputs results in substantial anthropogenic  $\text{N}_2\text{O}$  emissions from river networks, even though <1% of denitrified  $\text{NO}_3^-$  was converted to  $\text{N}_2\text{O}$ , a much lower percentage than has been reported for upland or flooded soils. Management efforts to enhance stream denitrification will reduce the delivery of N to sensitive coastal waters with less con-

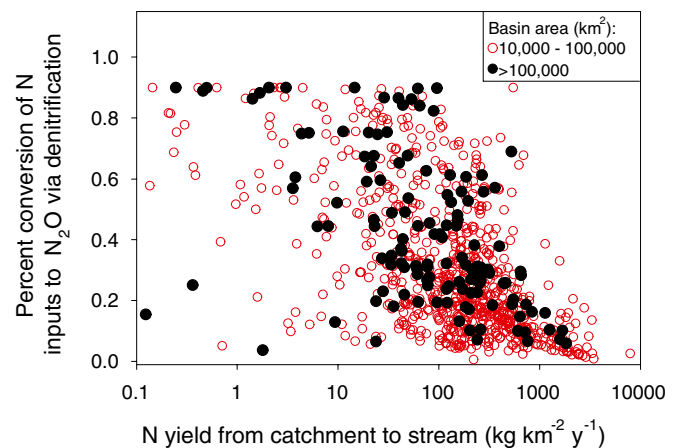


**Fig. 4.** Relationship between the percentage of dissolved inorganic nitrogen (DIN) inputs to river networks that are converted to  $\text{N}_2\text{O}$  via denitrification and the amount of DIN delivered to the river network from the catchment. Data are from 866 river networks included in a global river network model. Data points are split into rivers draining basins  $>100,000 \text{ km}^2$  (solid black circles) and those draining between  $10,000$  and  $100,000 \text{ km}^2$  (open red circles).

comitant N<sub>2</sub>O emissions than the enhancement of a comparable amount of denitrification in soils. Unfortunately, river networks have a limited capacity to remove NO<sub>3</sub><sup>-</sup> from the water column and anthropogenic N inputs have already overwhelmed this capacity in many river systems (33, 34). Whereas the trade-off between desirable N removal and undesirable N<sub>2</sub>O production may be smaller in streams than in soils, the best way to reduce N export to coastal waters without enhancing N<sub>2</sub>O emissions is to reduce N inputs to watersheds.

## Materials and Methods

LINX II consisted of <sup>15</sup>NO<sub>3</sub><sup>-</sup> additions to 72 small streams distributed across three land-use categories and eight regions to provide in situ measurements of N<sub>2</sub> and N<sub>2</sub>O production via denitrification at the whole-stream scale. We used a standardized set of experimental protocols to measure biogeochemical process rates including denitrification, ecosystem respiration, and gross primary production (35). We also measured a broad suite of physicochemical characteristics including organic matter standing stocks, water column nutrient concentrations, effective stream depth, stream width, stream discharge, and water velocity. The experiments were conducted as previously described (22, 35, 36) and as reported online in the project protocols (<http://www.biol.vt.edu/faculty/webster/linx/>). A detailed description of the experimental protocols, study site locations, and characteristics can be found in *SI Materials and Methods*, Fig. S1, and Table S1.

**Site Selection.** Study sites were selected to encompass a broad range of conditions across three land-use categories and eight regions. Within each region headwater streams (discharge ranged from 0.2–268 L s<sup>-1</sup>) were selected draining basins dominated by native vegetation (reference), urban land use, or agricultural land use, with three sites in each land use for a total of nine sites per region (Table S1, Fig. S1). We selected stream reaches that had minimal groundwater or surface water inputs and were long enough to allow for a measureable amount of in-stream N processing (105–1,830 m).

**Isotope Addition and Sampling.** The production of N<sub>2</sub> and N<sub>2</sub>O via denitrification was measured by continuously adding a solution of sodium bromide (NaBr, conservative tracer) and <sup>15</sup>N-enriched potassium nitrate (K<sup>15</sup>NO<sub>3</sub><sup>-</sup>, 98+% <sup>15</sup>N) to each stream for 24 h beginning at ≈13:00 hours using a small pump. The pump rate and injectate concentration were chosen to increase the stream water δ<sup>15</sup>N<sub>NO<sub>3</sub><sup>-</sup> by 20,000‰ and the Br<sup>-</sup> concentration by 100 μg L<sup>-1</sup>. The conservative tracer was used to account for ground and surface water inputs to the reach and to measure channel hydraulic properties. The K<sup>15</sup>NO<sub>3</sub><sup>-</sup> addition resulted in a relatively small (~7.5%) increase in stream water NO<sub>3</sub><sup>-</sup> concentration.</sub>

Ten sampling stations were selected along the study reach and water samples were taken for NO<sub>3</sub><sup>-</sup> (concentration and δ<sup>15</sup>N), N<sub>2</sub> (δ<sup>15</sup>N), and N<sub>2</sub>O (concentration and δ<sup>15</sup>N) several hours before, 12 h after, and 23 h after the K<sup>15</sup>NO<sub>3</sub><sup>-</sup> addition began. Nitrate samples were filtered (GFF; 0.7-μm pore size; Whatman) in the field and stored on ice or frozen before analysis. Our protocol for dissolved gas sampling is described in detail elsewhere (37) and is briefly outlined here. Gas samples were taken by slowly withdrawing 40 or 120 mL of stream water into a 60- or 140-mL polypropylene syringe (BD Falcon and Harvard Apparatus) equipped with a polycarbonate stopcock. Twenty mL of ultrahigh purity helium was then added to the syringes, which were gently shaken for 5 min to equilibrate the dissolved N<sub>2</sub> and N<sub>2</sub>O between the aqueous and gas phases. The headspace gas was then transferred to a preevacuated 12-mL Exetainer (Labco) and stored underwater before analysis. All gas transfers were done underwater to minimize contamination from atmospheric N<sub>2</sub> and N<sub>2</sub>O.

**Air–Water Gas Exchange Rate Measurement.** Within 1 d of the <sup>15</sup>NO<sub>3</sub><sup>-</sup> addition the air–water gas exchange rate ( $k_2$ , units of time<sup>-1</sup>) was measured using the steady-state tracer gas injection method with either propane or SF<sub>6</sub> as tracers (Table S1) (38, 39). The tracer gas and a conservative tracer [e.g., sodium chloride (NaCl) or rhodamine] were added to the stream at a constant rate. Water samples were collected from each of the 10 downstream sampling stations after the tracer concentrations reached a plateau throughout the reach as indicated by conductivity or fluorescence at the

most downstream sampling station. Gas tracer samples were collected in 5-mL polypropylene syringes and injected into preevacuated glass storage vials. The air–water gas exchange rate was calculated from the dilution-corrected decline in tracer gas concentration across the experimental reach (Table S1).

**Analytical Methods.** <sup>15</sup>N-NO<sub>3</sub> was determined on filtered water samples following Sigman et al. (40). Samples were analyzed for <sup>15</sup>N on a Finnigan Delta-5 or a Europa 20/20 mass spectrometer in the Mass Spectrometer Laboratory of the Marine Biological Laboratory in Woods Hole, MA (<http://ecosystems.mbl.edu/SILAB/about.html>); a Europa Integra mass spectrometer in the Stable Isotope Laboratory of the University of California, Davis, CA (<http://stableisotopefacility.ucdavis.edu/>); or a ThermoFinnigan DeltaPlus mass spectrometer in the Stable Isotope Laboratory at Kansas State University, Manhattan, KS (<http://www.k-state.edu/simsl>).

Gas samples were analyzed for δ<sup>15</sup>N<sub>2</sub>, δ<sup>15</sup>N<sub>2</sub>O, and N<sub>2</sub>O concentration by mass spectrometry using either a Europa Hydra Model 20/20 mass spectrometer at the Stable Isotope Laboratory of the University of California, Davis, CA, or a GV Instruments Prism Series II mass spectrometer in the Biogeochemistry Laboratory, Department of Zoology, Michigan State University, East Lansing, MI. The original stream water N<sub>2</sub>O concentration was calculated using temperature-corrected Bunsen solubility coefficients, a mass balance of the gas–liquid system in the sample syringe, and an atmospheric N<sub>2</sub>O partial pressure of 315 ppbv (41). Propane and SF<sub>6</sub> concentrations were measured using gas chromatography with flame ionization and electron capture detectors, respectively.

<sup>15</sup>N content of all samples was reported in δ<sup>15</sup>N notation, where δ<sup>15</sup>N = [(R<sub>SA</sub>/R<sub>ST</sub>) - 1] × 1,000, R = <sup>15</sup>N/<sup>14</sup>N, and the results are expressed as per mil deviation of the sample (SA) from the standard (ST), N<sub>2</sub> in air (δ<sup>15</sup>N = 0‰). All δ<sup>15</sup>N values were converted to <sup>15</sup>N mole fractions (MF = <sup>15</sup>N/<sup>14</sup>N + <sup>15</sup>N), and tracer <sup>15</sup>N fluxes were calculated for each sample by multiplying the <sup>15</sup>N MF, corrected for natural abundances of <sup>15</sup>N by subtracting the average <sup>15</sup>N MF for samples collected before the <sup>15</sup>N addition, by the concentrations of NO<sub>3</sub><sup>-</sup>, N<sub>2</sub>, or N<sub>2</sub>O in stream water (concentrations of NO<sub>3</sub><sup>-</sup> and N<sub>2</sub>O were measured, whereas N<sub>2</sub> was taken as the concentration in equilibrium with air at the ambient stream temperature) and stream discharge derived from the measured conservative solute tracer concentrations.

**Gas Production and Emission Calculations.** Rates of N<sub>2</sub> and N<sub>2</sub>O production were calculated as best-fit model parameters from a two-compartment model of denitrification linking <sup>15</sup>N<sub>2</sub>, <sup>15</sup>N<sub>2</sub>O, and <sup>15</sup>NO<sub>3</sub><sup>-</sup> over the study reach described in *SI Materials and Methods*. Nitrous oxide emission rates via diffusive evasion ( $F$ , μg N<sub>2</sub>O-N-m<sup>-2</sup>·h<sup>-1</sup>) were calculated as

$$F = k_2 \times h \times (N_2O_{\text{obs}} - N_2O_{\text{equil}}),$$

where  $h$  is the stream depth, N<sub>2</sub>O<sub>obs</sub> is the measured concentration of dissolved N<sub>2</sub>O in the water (average across all sampling stations), and N<sub>2</sub>O<sub>equil</sub> is the N<sub>2</sub>O concentration expected if the stream were in equilibrium with the atmosphere.

**Global River Network N<sub>2</sub>O Emission Model.** Global anthropogenic N<sub>2</sub>O emissions from river networks were estimated using a river network model. The model was run under mean annual conditions and accounts for the spatial distribution of DIN loading, temperature, hydrology, and denitrification efficiency loss. Model details and prediction errors can be found in Fig. S2 and *SI Materials and Methods*.

**ACKNOWLEDGMENTS.** We are grateful to N. E. Ostrom for assistance with stable isotope measurements of N<sub>2</sub> and N<sub>2</sub>O and G. P. Robertson for comments on the manuscript. We thank the US Forest Service, National Park Service, and many private landowners for permission to conduct experiments on their lands. We also acknowledge the many workers who helped with the Lotic Intersite Nitrogen experiments. Funding for this research was provided by the National Science Foundation (DEB-0111410). The National Science Foundation's Long Term Ecological Research (NSF-LTER) network hosted many of the study sites included in this research and partially supported several of the authors during the project. We specifically acknowledge Andrews, Central Arizona-Phoenix, Coweeta, Kellogg Biological Station, Konza, Luquillo, Plum Island, and Sevilleta NSF-LTERs for support.

- Robertson GP, Vitousek PM (2009) Nitrogen in Agriculture: Balancing the cost of an essential resource. *Annu Rev Environ Resour* 34:97–125.
- Forster P, et al. (2007) Changes in atmospheric constituents and in radiative forcing. *Climate Change 2007: The Physical Science Basis. Contributions of Working Group I to*

*the Fourth Assessment Report of the Intergovernmental Panel on Climate Change*, eds Solomon S, et al. (Cambridge Univ Press, New York).

- Ravishankara AR, Daniel JS, Portmann RW (2009) Nitrous oxide (N<sub>2</sub>O): The dominant ozone-depleting substance emitted in the 21st century. *Science* 326:123–125.

4. Stehfest E, Bouwman L (2006) N<sub>2</sub>O and NO emission from agricultural fields and soils under natural vegetation: Summarizing available measurement data and modeling of global annual emissions. *Nutr Cycl Agroecosyst* 74:207–228.
5. Firestone MK, Davidson EA (1989) Microbiological basis of NO and N<sub>2</sub>O production and consumption in soil. *Exchange of Trace Gases Between Terrestrial Ecosystems and the Atmosphere*, eds Andreae MO, Schimel DS (Wiley, Chichester, UK), pp 7–21.
6. Codispoti LA (2010) Oceans. Interesting times for marine N<sub>2</sub>O. *Science* 327:1339–1340.
7. Cole JJ, Caraco NF (2001) Emissions of nitrous oxide (N<sub>2</sub>O) from a tidal, freshwater river, the Hudson River, New York. *Environ Sci Technol* 35:991–996.
8. Beaulieu JJ, Arango CP, Hamilton SK, Tank JL (2008) The production and emission of nitrous oxide from headwater streams in the midwestern USA. *Glob Chang Biol* 14: 878–894.
9. Seitzinger SP, Kroeze C (1998) Global distribution of nitrous oxide production and N inputs in freshwater and coastal marine ecosystems. *Global Biogeochem Cycles* 12: 93–113.
10. Stevens RJ, Laughlin RJ, Malone JP (1998) Measuring the mole fraction and source of nitrous oxide in the field. *Soil Biol Biochem* 30:541–543.
11. Stevens RJ, Laughlin RJ (1998) Measurement of nitrous oxide and di-nitrogen emissions from agricultural soils. *Nutr Cycl Agroecosyst* 52:131–139.
12. Alexander RB, Boyer EW, Smith RA, Schwarz GE, Moore RB (2007) The role of headwater streams in downstream water quality. *J Am Water Resour Assoc* 43:41–59.
13. Groffman PM, et al. (2006) Methods for measuring denitrification: Diverse approaches to a difficult problem. *Ecol Appl* 16:2091–2122.
14. Burgin A, Hamilton SK (2007) Have we overemphasized the role of denitrification in aquatic ecosystems? A review of nitrate removal pathways. *Front Ecol Environ* 5: 89–96.
15. Firestone MK, Firestone RB, Tiedje JM (1980) Nitrous oxide from soil denitrification: Factors controlling its biological production. *Science* 208:749–751.
16. Firestone MK, Smith MS, Firestone RB, Tiedje JM (1979) The influence of nitrate, nitrite, and oxygen on the composition of the gaseous products of denitrification in soil. *Soil Sci Soc Am J* 43:1140–1144.
17. Hutchinson GL, Davidson EA (1993) Processes for production and consumption of gaseous nitrous oxide in soil. *Agricultural Ecosystem Effects on Trace Gases and Global Climate Change*, eds Harper LA, Mosier AR, Duxbury JM, Rolston DE (Am Soc Agron, Madison, WI), pp 79–94.
18. Swerts M, Merckx R, Vlassak K (1996) Denitrification, N<sub>2</sub>-fixation and fermentation during anaerobic incubation of soils amended with glucose and nitrate. *Biol Fertil Soils* 23:229–235.
19. Miller MN, et al. (2008) Crop residue influence on denitrification, N<sub>2</sub>O emissions and denitrifier community abundance in soil. *Soil Biol Biochem* 40:2553–2562.
20. Tiedje JM (1988) Ecology of denitrification and dissimilatory nitrate reduction to ammonium. *Biology of Anaerobic Microorganisms*, ed Zehnder AJB (Wiley, New York), pp 179–244.
21. Craig LS, et al. (2008) Stream restoration strategies for reducing river nitrogen loads. *Front Ecol Environ* 6:529–538.
22. Mulholland PJ, et al. (2008) Stream denitrification across biomes and its response to anthropogenic nitrate loading. *Nature* 452:202–205.
23. Schlesinger WH, Reckhow KH, Bernhardt ES (2006) Global change: The nitrogen cycle and rivers. *Water Resour Res* 42:W03S06.
24. Laursen AE, Seitzinger SP (2004) Diurnal patterns of denitrification, oxygen consumption and nitrous oxide production in rivers measured at the whole-reach scale. *Freshw Biol* 49:1448–1458.
25. Seitzinger S, et al. (2006) Denitrification across landscapes and waterscapes: A synthesis. *Ecol Appl* 16:2064–2090.
26. Holmes RM, Jones JB, Fisher SG, Grimm NB (1996) Denitrification in a nitrogen-limited stream ecosystem. *Biogeochemistry* 33:125–146.
27. Webster JR, et al. (2003) Factors affecting ammonium uptake in streams—an inter-biome perspective. *Freshw Biol* 48:1329–1352.
28. Arango CP, Tank JL (2008) Land use influences the spatiotemporal controls of nitrification and denitrification in headwater streams. *J North Am Benthol Soc* 27: 90–107.
29. Richardson WB, et al. (2004) Denitrification in the Upper Mississippi River: Rates, controls, and contribution to nitrate flux. *Can J Fish Aquat Sci* 61:1102–1112.
30. Mosier A, et al. (1998) Closing the global N<sub>2</sub>O budget: Nitrous oxide emissions through the agricultural nitrogen cycle—OECD/IPCC/IEA phase II development of IPCC guidelines for national greenhouse gas inventory methodology. *Nutr Cycl Agroecosyst* 52:225–248.
31. Seitzinger SP, Kroeze C, Styles RV (2000) Global distribution and N<sub>2</sub>O emissions from aquatic systems: Natural emissions and anthropogenic effects. *Chemosphere Glob Chang Sci* 2:267–279.
32. Wollheim WM, et al. (2008) Global N removal by freshwater aquatic systems using a spatially distributed, within-basin approach. *Global Biogeochem Cycles* 22:GB2026.
33. Caraco NF, Cole JJ (1999) Human impact on nitrate export: An analysis using major world rivers. *Ambio* 28:167–170.
34. Bernot MJ, Dodds WK (2005) Nitrogen retention, removal, and saturation in lotic ecosystems. *Ecosystems (N Y)* 8:442–453.
35. Bernot MJ, et al. (2010) Inter-regional comparison of land-use effects on stream metabolism. *Freshw Biol* 55:1874–1890.
36. Mulholland PJ, et al. (2009) Nitrate removal in stream ecosystems measured by <sup>15</sup>N addition experiments: Denitrification. *Limnol Oceanogr* 54:666–680.
37. Hamilton SK, Ostrom NE (2007) Measurement of the stable isotope ratio of dissolved N<sub>2</sub> in <sup>15</sup>N tracer experiments. *Limnol Oceanogr Methods* 5:233–240.
38. Genereux DP, Hemond HF (1992) Determination of gas-exchange rate constants for a small stream on Walker Branch Watershed, Tennessee. *Water Resour Res* 28: 2365–2374.
39. Wanninkhof R, Mulholland PJ, Elwood JW (1990) Gas-exchange rates for a 1st-order stream determined with deliberate and natural tracers. *Water Resour Res* 26:1621–1630.
40. Sigman DM, et al. (1997) Natural abundance-level measurement of the nitrogen isotopic composition of oceanic nitrate: An adaptation of the ammonia diffusion method. *Mar Chem* 57:227–242.
41. Weiss RF, Price BA (1980) Nitrous oxide solubility in water and seawater. *Mar Chem* 8: 347–359.

# Supporting Information

Beaulieu et al. 10.1073/pnas.1011464108

## SI Materials and Methods

The experiments for the second Lotic Intersite Nitrogen experiment (LINX II) were conducted as previously described (1, 2) and as reported online in the project protocols (<http://www.biol.vt.edu/faculty/webster/linx/>).

**Site Selection.** Drainage basin boundaries for each stream above the bottom of the experimental reach were delineated from 30-m raster digital elevation models [US Geological Survey (USGS) National Elevation Data Set, available at <http://seamless.usgs.gov>], using the Spatial Analyst extension in ArcView GIS software (Version 3.3; Environmental Systems Research Institute). Before delineating basins, elevation datasets were modified by lowering the elevation values of pixels associated with mapped stream channels to force flow direction maps to match existing 1:24,000-scale hydrography (3). Land cover in each basin was determined from the 30-m resolution 2001 USGS National Land Cover Datasets (NLCD; available online at <http://seamless.usgs.gov>), except that land cover for Puerto Rico (PR) was from 1991–1992 Landsat Thematic Mapper imagery (4) because the NLCD 2001 data were not available for all of our streams. Land cover data were reclassified as native (all forest, shrubland, grassland, and wetland categories), agricultural (all pasture, crop, orchard/vineyard, and fallow categories), or urban (all industrial, commercial, residential, transportation, and recreational turfgrass categories).

**Air–Water Gas Exchange Rate Calculations.** The air–water gas exchange rate ( $k_2$ ) was calculated from the tracer gas addition data using the model

$$\ln[\text{tracer gas}]_x = \ln[\text{tracer gas}]_0 - (a \times x), \quad [\text{S1}]$$

where  $[\text{tracer gas}]_x$  is the tracer gas concentration (e.g., propane or SF<sub>6</sub>) at a point  $x$  m downstream from the addition site and  $[\text{tracer gas}]_0$  is the concentration at the most upstream station, and  $a$  is the rate constant for tracer gas loss (i.e., diffusive evasion) per meter of stream channel that was multiplied by water velocity to yield  $k_2$  in units (d<sup>-1</sup>). Tracer gas concentrations were corrected for dilution by lateral inflows on the basis of the conservative solute tracer data collected at each station. Air–water gas exchange rates were converted from propane or SF<sub>6</sub> to N<sub>2</sub>, N<sub>2</sub>O, and O<sub>2</sub> using the ratio of their Schmidt numbers (5, 6). The effect of water temperature on  $k_2$  was accounted for using the relationship of Elmore and West (7).

**N Gas Production Rate Calculations.** N<sub>2</sub> and N<sub>2</sub>O production rates were estimated by fitting a model of N gas production to the measured fluxes of tracer <sup>15</sup>N as N<sub>2</sub> and N<sub>2</sub>O over the study reach as

$$d^{15}\text{N}_{\text{GAS}}/dx = k_{\text{N}_{\text{gas}}}^{15}\text{NO}_3 - k_2^{15}\text{N}_{\text{GAS}}, \quad [\text{S2}]$$

where <sup>15</sup>NO<sub>3</sub> is the tracer <sup>15</sup>N flux in NO<sub>3</sub><sup>-</sup> (μg <sup>15</sup>N·s<sup>-1</sup>) and <sup>15</sup>N<sub>GAS</sub> is the tracer <sup>15</sup>N flux in N<sub>2</sub> or N<sub>2</sub>O (ng <sup>15</sup>N·s<sup>-1</sup>),  $k_{\text{N}_{\text{gas}}}$  is the distance-specific N<sub>2</sub> or N<sub>2</sub>O production rate (m<sup>-1</sup>), and  $k_2$  is the air–water exchange rate of N<sub>2</sub> or N<sub>2</sub>O. The equation was solved for  $k_{\text{N}_2}$  and  $k_{\text{N}_2\text{O}}$  using the optimization tool “Solver” in Microsoft Office Excel.

Confidence intervals were determined for all  $k_{\text{N}_2}$  and  $k_{\text{N}_2\text{O}}$  values using maximum-likelihood analysis (MLE) and we retained estimates only from sites where the confidence interval did not

overlap zero (8). This procedure resulted in the determination of  $k_{\text{N}_2}$  for 49 streams,  $k_{\text{N}_2\text{O}}$  for 53 streams, and both  $k_{\text{N}_2}$  and  $k_{\text{N}_2\text{O}}$  for 40 streams. The N<sub>2</sub>O yield was calculated as

$$\text{N}_2\text{O yield (\%)} = \frac{k_{\text{N}_2\text{O}}}{k_{\text{N}_2\text{O}} + k_{\text{N}_2}} \times 100. \quad [\text{S3}]$$

Areal N<sub>2</sub> and N<sub>2</sub>O production rates ( $U$ , μg N·m<sup>-2</sup>·h<sup>-1</sup>) were calculated as  $U = ((k_{\text{N}_{\text{gas}}} \times \text{NO}_3^- \text{-N flux})/w) \times 3,600 \text{ s}\cdot\text{h}^{-1}$ , where NO<sub>3</sub><sup>-</sup>-N flux was determined from NO<sub>3</sub><sup>-</sup> concentration and discharge, and  $w$  is wetted width (meters).

Denitrification and N<sub>2</sub>O production rates reported for each stream are the average of the rates measured for the two sampling periods. Differences in  $k$  for both N<sub>2</sub> and N<sub>2</sub>O production between day and night were not statistically significant.

**Physical, Chemical, and Functional Stream Characteristics.** Water samples were analyzed for concentrations of NO<sub>3</sub><sup>-</sup> (either by ion chromatography or by azo dye colorimetry after Cd–Cu reduction), NH<sub>4</sub> (by phenate colorimetry or fluorometry), total soluble N (TSN, by high-temperature combustion; TOC-V with Total Nitrogen Module; Shimadzu), soluble reactive phosphorus (SRP, by ascorbic acid–molybdenum blue colorimetry), and dissolved organic carbon (DOC, by high-temperature combustion; TOC-V; Shimadzu) (Table S1).

Discharge ( $Q$ ) was estimated from the concentration of the Br<sup>-</sup> tracer in the stream, the injectate Br<sup>-</sup> concentration, and the injection rate. Stream velocity ( $v$ ) was measured from the rising limb of the conservative tracer at the bottom of the experimental reach. Stream depth ( $h$ ) was calculated as

$$h = \frac{Q}{w \times v}, \quad [\text{S4}]$$

where  $w$  is width that was measured at 5- to 10-m intervals along the experimental reach.

Standing stocks of select biomass compartments such as aquatic vascular plants and fine benthic organic matter were estimated by collecting material from a known area of the stream bottom and measuring both dry mass and ash-free dry mass (AFDM) (9). Whole ecosystem stream metabolism was measured with the diel dissolved oxygen method (10).

**Statistical Analysis.** To improve normality before parametric statistical analysis most data were log<sub>10</sub> transformed. Nitrous oxide emission rates were log( $x + 100$ ) transformed due to negative values. Simple and multiple linear regression was used to detect relationships between dependent and independent variables (e.g., N<sub>2</sub>O emission rate vs. NO<sub>3</sub><sup>-</sup>). Effect of land use category was determined using ANOVA or the Kruskal–Wallis nonparametric test. Differences between daytime and nighttime N<sub>2</sub>O emission rates were determined using  $t$  tests. A threshold in the relationship between N<sub>2</sub>O emission rate and streamwater NO<sub>3</sub><sup>-</sup> was tested for using a 2D Kolmogorov–Smirnov test (11). The test was performed using software available at <http://www.zoology.siu.edu/garvey/2dks.html>. All other statistical tests were performed using SYSTAT, Version 12 for Windows (SYSTAT Software).

**Stream Network Model Development and Application.** We modified an existing global river network N removal model (12) to estimate global N<sub>2</sub>O production via denitrification in river systems. The model is applied to mean annual conditions in the contemporary period (corresponding roughly with mid-1990s) and accounts for

the spatial distribution of aquatic dissolved inorganic nitrogen (DIN) loading relative to discharge conditions, temperature, and aquatic ecosystem dimensions and types within the river network. The major modifications from the earlier model are (i) to account for efficiency loss of the denitrification process (1) rather than assume a linear denitrification response to increasing concentration, (ii) to apply aquatic DIN loading rates to aquatic systems using the model of Green et al. (13) rather than aquatic total nitrogen (TN) loading using the model of Bouwman et al. (14), and (iii) to use river DIN rather than TN observations (15) to assess model predictions. Both the DIN loading dataset and the observed DIN concentrations at river basin mouths are for the same time period (mid-1990s). All other characteristics, such as river network geomorphology (including the statistical representation of small river geomorphology and routing), discharge, channel hydraulic assumptions, lake/reservoir distribution, and temperature are identical to the earlier model (12). We briefly summarize the overall model approach, the modifications, and the comparison of model predictions with observations.

**Model equations.** We use a 30-min global river network (STN-30) (16) modified to integrate small rivers as well as lakes and reservoirs along river systems. Mean annual denitrification is calculated in each water body along all surface water flow paths, accounting for sequential removal and changing conditions as water flows from source areas downstream. DIN flux exported from each grid cell  $i$  ( $\text{kg}\cdot\text{y}^{-1}$ ) is determined as

$$\text{DIN}_i = (\text{LocalPoint}_i + (\text{LocalNonPoint}_i \times \text{TE}_{\text{localriver},i}) + \text{UpstreamIn}_i) \times \text{TE}_{\text{largeriver},i} \times \text{TE}_{\text{lake},i} \times \text{TE}_{\text{reservoir},i}, \quad [\text{S5}]$$

where LocalPoint is all point sources in grid cell  $i$  ( $\text{kg}\cdot\text{y}^{-1}$ ); LocalNonPoint is all nonpoint N inputs to the aquatic system in  $i$  ( $\text{kg}\cdot\text{y}^{-1}$ ); UpstreamIn is DIN inputs from all grid cells immediately upstream from  $i$  ( $\text{kg}\cdot\text{y}^{-1}$ ); and TE is transfer efficiency [ $\text{TE} = 1 - R$ , where  $R$  is the proportion of inputs removed by the water body (unitless)] associated with the local river network, large river channels, lakes, and/or reservoirs within the grid cell.

TE for each water body is calculated as

$$\text{TE} = \exp\left(\frac{-v_f}{H_L}\right), \quad [\text{S6}]$$

where  $v_f$  represents biological activity in the form of the uptake velocity or mass transfer coefficient of the nutrient ( $\text{m}\cdot\text{y}^{-1}$ ; see below) and  $H_L$  represents hydrological conditions in the form of the hydraulic load ( $\text{m}\cdot\text{y}^{-1}$ ). Hydraulic load is calculated as  $Q/A$ , where  $Q$  is discharge into the water body ( $\text{m}^3\cdot\text{y}^{-1}$ ), and  $A$  is benthic surface area [width  $\times$  length in riverine systems ( $\text{m}^2$ )].

**DIN loading to aquatic ecosystems.** DIN loading is based on spatially distributed (half-degree resolution), annual estimates of nitrogen inputs onto land via net fertilizer applications (i.e., surplus after harvest), atmospheric deposition, and animal waste and directly to water via point sources. Transfer of nonpoint sources from land to water as DIN is based on terrestrial transfer parameters calibrated at the basin scale (13). Transfer from land to water is governed by runoff coefficients, air temperature, and water residence time in the soils. We estimated spatially distributed nonpoint DIN inputs to aquatic ecosystems using the spatially distributed estimates of net N inputs (pixel level) and basin-level transfer efficiencies. In our model, we assume that point sources are deposited directly into large rivers or lakes (i.e., they bypass small subgrid cell rivers that receive only nonpoint inputs) as in ref. 12.

**Modeled uptake velocities.** We used the efficiency loss model for denitrification recently derived from LINX II (1) to calculate denitrification uptake velocities on the basis of N concentrations in every grid cell. The streams in the LINX experiments ( $n = 72$ )

encompassed a wide range of North American biomes, land uses, and nitrate concentrations ( $<0.01$ – $20 \text{ mg}\cdot\text{L}^{-1}$ ). All were first- or second-order streams ( $Q < 268 \text{ L}\cdot\text{s}^{-1}$ ), measured during the warmer half of the year. Nitrate concentrations were found to be the primary determinant of denitrification rates. The power function describing the relationship was applied,

$$\log v_f = -0.493 \log[\text{NO}_3^-] - 2.975, \quad [\text{S7}]$$

where  $v_f$  is denitrification uptake velocity ( $\text{cm}\cdot\text{s}^{-1}$ ), and  $\text{NO}_3^-$  is nitrate concentration ( $\mu\text{g NO}_3^- \cdot \text{N}\cdot\text{L}^{-1}$ ). In each grid cell, DIN concentrations (presumed to be primarily  $\text{NO}_3^-$ ) were calculated on the basis of inputs from the upstream grid cell and local inputs. Thus, upstream removal affects the calculated denitrification in each local grid cell. Because most of the  $^{15}\text{N}$  denitrification experiments were conducted during warm seasons, we used a  $Q_{10}$  approach to scale  $v_f$  to mean annual water temperature in each grid cell globally, assuming  $T_{\text{ref}} = 20^\circ\text{C}$  and  $Q_{10} = 2$ . We assumed that this efficiency loss model was generally applicable to all aquatic systems (rivers, lakes, and reservoirs). This is a reasonable first approximation of denitrification rates globally, given that denitrification rates follow similar patterns in riverine and lacustrine systems (17). We applied the denitrification  $\text{N}_2\text{O}$  yield as reported in the text (i.e., 0.9% of denitrified  $\text{NO}_3^- \cdot \text{N}$  converted to  $\text{N}_2\text{O}$ ) to calculate  $\text{N}_2\text{O}$  production via denitrification in each grid cell.

**Model prediction vs. observation.** All parameter values in the network removal model were based on empirical results (e.g., Eq. S7) or a priori assumption (i.e., no tuning was performed). We compared predicted and observed DIN areal exports ( $\text{kg}\cdot\text{km}^{-2}\cdot\text{y}^{-1}$ ) at the basin mouth for 96 large watersheds distributed globally. Median prediction error ( $\text{PE} = [\text{Predicted} - \text{Observed}]/\text{Observed} \times 100$ ) (18) is 42% ( $-22$ – $169\%$  interquartile range), compared with 151% ( $43$ – $364\%$  interquartile range) if no aquatic denitrification is assumed (i.e., only mixing of aquatic DIN loads). Overall, our model tends to overpredict fluxes at basin mouths (Wilcoxon signed ranks test on log-transformed areal flux data;  $P = 0.003$ ) and therefore likely underpredicts denitrification and  $\text{N}_2\text{O}$  production. This result is expected, given that we do not account for all aquatic removal processes (e.g., indirect denitrification and long-term storage in depositional zones). However, errors may also be attributed to other sources, including the DIN loading model as well as the observations of mean annual exports from basin mouths. Nevertheless, we expect our global estimates of  $\text{N}_2\text{O}$  production via denitrification by aquatic ecosystems to be conservative. Overall, the model explains 49% of the variability in observations. There is a tendency for predictions to be higher than observed in basins with higher N fluxes, resulting in a slope between predicted and observed of  $<1$  [ $\log(\text{Observed}) = 0.80 + 0.55 \log(\text{Predicted})$ ,  $n = 96$ ; dashed line in Fig. S2]. The relationship between observed and predicted is improved if a few basins with low predicted DIN flux ( $<10 \text{ kg}\cdot\text{km}^{-2}\cdot\text{y}^{-1}$ ) are excluded [ $\log(\text{Observed}) = 0.17 + 0.83 \log(\text{Predicted})$ ,  $n = 86$ ,  $r^2 = 0.59$ ; red line in Fig. S2].

**Global  $\text{N}_2\text{O}$  Budget.** We estimated global anthropogenic  $\text{N}_2\text{O}$  emissions from river systems using the IPCC methodology described in Mosier et al. (19) and our emission factor for river systems. The calculations are described below using the IPCC nomenclature:

$$\text{N}_2\text{O production within river systems} = \text{NLEACH} \times (\text{EF5-r}). \quad [\text{S8}]$$

NLEACH is the amount of N fertilizer and manure that enters river networks from leaching and EF5-r is the fraction of NLEACH that is converted to  $\text{N}_2\text{O}$  within a river network. Our global river  $\text{N}_2\text{O}$  production model demonstrates that 0.25% of anthropogenic N inputs to river networks are converted to  $\text{N}_2\text{O}$

via denitrification. We adopted the IPCC's assumption that nitrification converts twice as much anthropogenic N to N<sub>2</sub>O as denitrification (e.g., 0.5%). Therefore, EF5-r is 0.75%.

NLEACH is defined as

$$\text{NLEACH} = [\text{NFERT} + \text{NEX}] \times \text{FRACLEACH}, \quad [\text{S9}]$$

where NFERT is global synthetic fertilizer use, NEX is the amount of N excreted by livestock globally, and FRACLEACH is the fraction of fertilizer and manure N lost to leaching and surface runoff (0.30). NFERT for 2007 was obtained from the United Nations Food and Agriculture Organization (FAO, [www.fao.org](http://www.fao.org)). NEX was estimated from livestock statistics for 2003 (FAO) and N excretion values per animal type and region as outlined by the IPCC (19). Using the most current data available, NLEACH was calculated as

$$\begin{aligned} \text{NLEACH} &= [109 \text{ Tg N} \cdot \text{y}^{-1} + 191 \text{ Tg N} \cdot \text{y}^{-1}] \times 0.3 \\ &= 90 \text{ Tg N} \cdot \text{y}^{-1} \end{aligned}$$

and combining this rate with the EF5-r estimate of 0.75% yields an estimated N<sub>2</sub>O production within global river systems of 0.68 Tg N·y<sup>-1</sup>.

**Figures.** The literature values in Fig. 1A came from refs. 20–24.

The data in Fig. 2 came from several sources. Data from soils came from two reviews (25, 26) and two additional studies (27, 28). Data from estuaries, lakes, and rivers came from ref. 22 and references therein. Data from streams came from this study and ref. 29.

- Mulholland PJ, et al. (2008) Stream denitrification across biomes and its response to anthropogenic nitrate loading. *Nature* 452:202–205.
- Mulholland PJ, et al. (2009) Nitrate removal in stream ecosystems measured by <sup>15</sup>N addition experiments: Denitrification. *Limnol Oceanogr* 54:666–680.
- King RS, et al. (2005) Spatial considerations for linking watershed land cover to ecological indicators in streams. *Ecol Appl* 15:137–153.
- Helmer EH, Ramos O, Lopez TD, Quinones M, Diaz W (2002) Mapping the forest type and land cover of Puerto Rico, a component of the Caribbean biodiversity hotspot. *Caribb J Sci* 38:165–183.
- MacIntyre S, Wanninkhof R, Chanton JP (1995) Trace gas exchange across the air-water interface in freshwater and coastal marine environments. Biogenic trace gases: Measuring emissions from soil and water. *Methods in Ecology*, eds Matson PA, Harris RC (Blackwell, London).
- Wanninkhof R (1992) Relationship between wind-speed and gas-exchange over the ocean. *J Geophys Res. Oceans* 97:7373–7382.
- Elmore HL, West WF (1961) Effect of temperature on stream reaeration. *J Sanit Eng Div ASCE* 87:59–71.
- Hilborn R, Mangel M (1997) *The Ecological Detective: Confronting Models with Data* (Princeton Univ Press, Princeton).
- Benfield EF (2006) Decomposition of leaf material. *Methods in Stream Ecology*, eds Hauer FR, Lamberti GA (Elsevier, San Diego), 2nd Ed, pp 711–720.
- Bott TL (2006) Primary productivity and community respiration. *Methods in Stream Ecology*, eds Hauer FR, Lamberti GA (Elsevier, Amsterdam), 2nd Ed, pp 663–690.
- Garvey JE, Marschall EA, Wright RA (1998) From star charts to stoneflies: Detecting relationships in continuous bivariate data. *Ecology* 79:442–447.
- Wollheim WM, et al. (2008) Global N removal by freshwater aquatic systems using a spatially distributed, within-basin approach. *Global Biogeochem Cycles* 22:GB2026.
- Green PA, et al. (2004) Pre-industrial and contemporary fluxes of nitrogen through rivers: A global assessment based on typology. *Biogeochemistry* 68:71–105.
- Bouwman AF, Van Drecht G, Knoop JM, Beusen AHW, Meinardi CR (2005) Exploring changes in river nitrogen export to the world's oceans. *Global Biogeochem Cycles* 19: B1002.
- Meybeck M, Ragu A (1995) *River Discharges to Oceans: An Assessment of Suspended Solids, Major Ions, and Nutrients* (United Nations Environmental Programme, Nairobi).
- Vörossmarty CJ, Fekete BM, Meybeck M, Lammers RB (2000) Geomorphometric attributes of the global system of rivers at 30-minute spatial resolution. *J Hydrol (Amst)* 237:17–39.
- Piña-Ochoa E, Álvarez-Cobelas M (2006) Denitrification in aquatic environments: A cross-system analysis. *Biogeochemistry* 81:111–130.
- Alexander RB, Johnes PJ, Boyer EW, Smith RA (2002) A comparison of models for estimating the riverine export of nitrogen from large watersheds. *Biogeochemistry* 57:295–339.
- Mosier A, et al. (1998) Closing the global N<sub>2</sub>O budget: Nitrous oxide emissions through the agricultural nitrogen cycle—OECD/IPCC/IEA phase II development of IPCC guidelines for national greenhouse gas inventory methodology. *Nutr Cycl Agroecosyst* 52:225–248.
- García-Ruiz R, Pattinson SN, Whitton BA (1998) Denitrification and nitrous oxide production in sediments of the Wiske, a lowland eutrophic river. *Sci Total Environ* 210:307–320.
- García-Ruiz R, Pattinson SN, Whitton BA (1999) Nitrous oxide production in the river Swale-Ouse, North-East England. *Water Res* 33:1231–1237.
- Seitzinger SP (1988) Denitrification in freshwater and coastal marine ecosystems: Ecological and geochemical significance. *Limnol Oceanogr* 33:702–724.
- Beaulieu JJ, Arango CP, Tank JL (2009) The effects of season and agriculture on nitrous oxide production in headwater streams. *J Environ Qual* 38:637–646.
- Smith R, Böhlke J, Repert D, Hart C (2009) Nitrification and denitrification in a midwestern stream containing high nitrate: In situ assessment using tracers in dome-shaped incubation chambers. *Biogeochemistry* 96:189–208.
- Schlesinger WH (2009) On the fate of anthropogenic nitrogen. *Proc Natl Acad Sci USA* 106:203–208.
- Stevens RJ, Laughlin RJ (1998) Measurement of nitrous oxide and di-nitrogen emissions from agricultural soils. *Nutr Cycl Agroecosyst* 52:131–139.
- Bergsma TT, Ostrom NE, Emmons M, Robertson GP (2001) Measuring simultaneous fluxes from soil of N<sub>2</sub>O and N<sub>2</sub> in the field Using the <sup>15</sup>N-gas “nonequilibrium” technique. *Environ Sci Technol* 35:4307–4312.
- Bergsma TT, Robertson GP, Ostrom NE (2002) Influence of soil moisture and land use history on denitrification end-products. *J Environ Qual* 31:711–717.
- Mulholland PJ, et al. (2004) Stream denitrification and total nitrate uptake rates measured using a field <sup>15</sup>N tracer addition approach. *Limnol Oceanogr* 49:809–820.

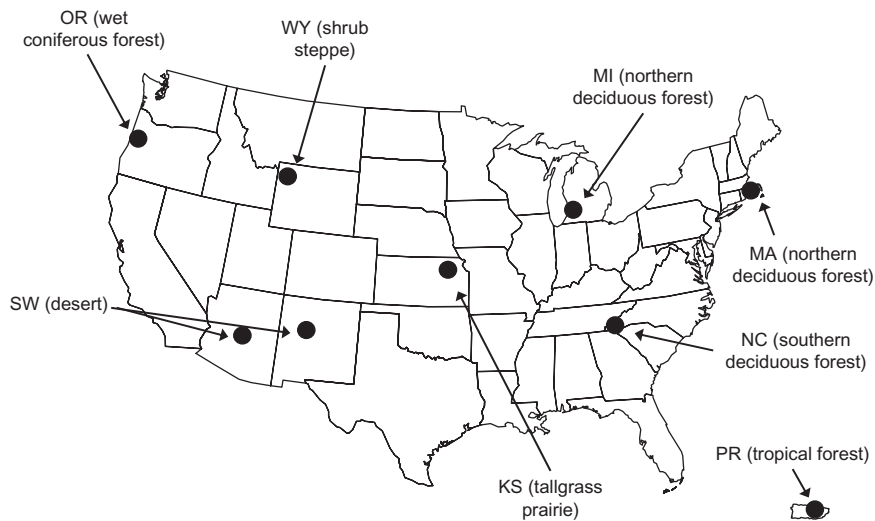


**Fig. S1.** General location of study sites and major biomes. Nine streams were located near each solid circle with the exception of the southwest where the nine sites were distributed between Arizona and New Mexico.

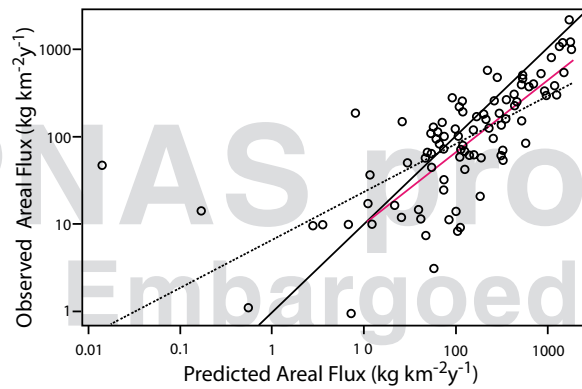


**Fig. S2.** Observed vs. predicted areal dissolved inorganic nitrogen (DIN) fluxes ( $\text{kg}\cdot\text{km}^{-2}\cdot\text{y}^{-1}$ ) from 96 global river basins. The solid line is the 1:1 line. The dotted line is the regression through all of the data. The red line is the regression through only those basins with predicted DIN fluxes  $>10 \text{ kg}\cdot\text{km}^{-2}\cdot\text{y}^{-1}$ .

Table S1. Location and mean physical, chemical, and biogeochemical characteristics of LINX II streams during the <sup>15</sup>N experiments

Region (biome)	Land use	NO <sub>3</sub> <sup>-</sup> , μg N·L <sup>-1</sup>	NH <sub>4</sub> <sup>+</sup> , μg N·L <sup>-1</sup>	SRP, μg P·L <sup>-1</sup>	DOC, mg·L <sup>-1</sup>	Discharge, L·s <sup>-1</sup>	Ave temp, °C	k <sub>2</sub> , d <sup>-1</sup>	Ecosystem respiration, g O <sub>2</sub> ·m <sup>-2</sup> ·d <sup>-1</sup>	N <sub>2</sub> O emission rate, μg N·m <sup>-2</sup> ·h <sup>-1</sup>	N <sub>2</sub> O yield, %	N <sub>2</sub> O production via denitrification, μg N·m <sup>-2</sup> ·h <sup>-1</sup>
KS (tallgrass prairie)	Agr	35	31.7	0.2	4.19	0.2	21.5	7	7.6	0.4	n.d.	0.13
	Agr	6	3.1	2.4	1.56	1	20.4	34	1.1	0.8	n.d.	0.01
	Agr	21162	3.4	16.2	2.42	5	20.8	20	2.8	541.4	0.98	89.44
	Ref	9	0.3	0.5	0.73	13	13.5	139	3.1	16.3	n.d.	n.d.
	Ref	1	6.7	1.9	0.77	26	17.4	54	2.6	12.8	n.d.	n.d.
	Ref	1	4.7	1.0	0.54	4	14.9	3	1.9	0.4	n.d.	n.d.
	Urb	2942	7.8	4.0	4.16	3	25.5	2	0.5	15.7	5.63	20.14
	Urb	277	28.3	35.4	3.81	2	27.1	19	6.7	31.0	0.08	2.78
	Urb	168	24.2	7.2	1.66	20	19.7	25	0.9	15.0	0.50	2.83
	MA (northern deciduous forest)	Agr	1164	80.2	7.8	2.10	1	16.3	9	11.0	15.1	1.56
Agr	989	63.1	10.8	3.46	2	16.6	45	8.2	9.3	0.35	14.01	
Agr	50	30.5	33.5	13.92	120	22.6	4	4.5	22.6	2.23	13.01	
Ref	15	293.2	1.5	8.70	5	17.9	3	3.8	1.0	n.d.	0.24	
Ref	53	13.3	9.2	6.80	12	19.8	36	14.6	10.2	0.23	0.74	
Ref	112	435.4	80.3	25.56	2	21.4	27	11.3	14.6	n.d.	n.d.	
Urb	1336	121.2	2.1	2.85	2	17.1	17	9.1	348.3	0.77	24.63	
Urb	513	253.8	11.8	12.47	11	18.7	43	4.0	140.5	1.49	38.97	
Urb	1025	39.2	11.5	10.03	5	21.2	8	1.2	23.3	0.95	10.33	
MI (northern deciduous forest)	Agr	4158	29.4	68.1	18.72	2	12.3	37	1.3	9.1	0.65	1.83
	Agr	82	20.7	11.3	8.22	6	17.9	220	5.6	-2.0	0.22	0.39
	Agr	1453	27.9	1.7	3.02	23	11.8	29	4.1	26.5	0.96	5.73
	Ref	283	54.8	14.9	4.30	5	15.1	102	2.0	20.2	0.43	3.04
	Ref	384	11.0	2.3	1.16	6	12.6	303	15.6	-18.2	0.09	2.13
	Ref	4	21.1	3.7	4.24	99	22.2	15	7.9	-4.5	n.d.	n.d.
	Urb	1100	127.7	9.2	2.36	35	12.4	33	8.7	53.5	0.45	14.12
	Urb	695	74.3	5.4	7.36	12	17.8	80	4.1	120.5	0.50	9.35
	Urb	274	32.0	10.7	2.80	110	20.0	17	14.1	13.9	0.24	4.48
	NC (southern deciduous forest)	Agr	154	17.1	2.8	0.58	53	17.6	17	1.6	14.3	n.d.
Agr	406	108.2	18.2	1.63	26	18.0	58	4.5	52.1	0.90	7.15	
Agr	173	8.5	6.7	0.81	189	16.1	138	8.7	253.4	0.49	3.35	
Ref	7	3.2	2.8	0.40	19	12.7	250	2.2	-25.0	n.d.	0.36	
Ref	241	5.6	2.5	0.49	12	14.7	68	3.4	6.4	0.09	0.22	
Ref	10	2.7	1.9	0.87	49	12.7	96	5.2	6.0	n.d.	0.63	
Urb	103	15.4	4.3	0.55	45	17.3	77	6.5	54.6	n.d.	4.53	
Urb	140	6.0	2.1	1.37	52	16.7	94	7.8	7.2	0.64	0.44	
Urb	54	2.6	2.9	0.93	80	13.8	192	17.9	6.0	n.d.	n.d.	

Table S1. Cont.

Region (biome)	Land use	NO <sub>3</sub> <sup>-</sup> , μg N L <sup>-1</sup>	NH <sub>4</sub> <sup>+</sup> , μg N L <sup>-1</sup>	SRP, μg P L <sup>-1</sup>	DOC, mg L <sup>-1</sup>	Discharge, L s <sup>-1</sup>	Ave temp, °C	k <sub>2</sub> , d <sup>-1</sup>	Ecosystem respiration, g O <sub>2</sub> m <sup>-2</sup> d <sup>-1</sup>	N <sub>2</sub> O emission rate, μg N m <sup>-2</sup> h <sup>-1</sup>	N <sub>2</sub> O yield, %	N <sub>2</sub> O production via denitrification, μg N m <sup>-2</sup> h <sup>-1</sup>
OR (wet coniferous forest)	Agr	96	8.4	47.8	10.08	6	17.3	4	1	2.7	0.67	0.32
	Agr	54	6.1	5.3	0.89	113	17.6	17	5	12.3	0.72	1.57
	Agr	97	10.6	5.0	2.57	35	18.9	9	4	6.1	0.54	4.64
	Ref	71	1.3	34.7	2.05	8	15.1	23	1	2.5	n.d.	n.d.
	Ref	63	5.9	13.0	0.88	31	12.5	201	5	3.2	n.d.	n.d.
	Ref	69	4.0	24.5	1.27	19	13.7	151	14	-4.0	n.d.	n.d.
	Urb	163	19.3	45.3	1.87	6	20.3	4	7	4.7	1.29	2.13
	Urb	2	4.8	17.8	3.45	25	21.1	24	5	2.7	n.d.	0.04
	Urb	8	4.4	208.5	7.04	3	22.6	n.d.	10	n.d.	n.d.	n.d.
	PR (tropical forest)	Agr	276	11.1	13.2	1.76	12	23.0	94	7.6	31.9	2.55
Agr	206	7.1	11.5	0.90	25	23.0	16	16	5.3	23.7	0.76	1.76
Agr	446	2.6	8.7	1.01	112	23.0	27	15.7	15.7	145.8	0.36	28.47
Ref	171	2.6	21.5	0.64	13	21.3	324	2.4	2.4	23.6	0.14	1.54
Ref	131	7.2	0.2	0.26	20	19.0	62	4.5	4.5	48.7	2.98	3.57
Ref	105	2.5	7.3	1.31	5	22.1	19	0.4	0.4	4.7	0.80	0.24
Urb	997	15.1	26.3	1.49	5	24.3	21	4.6	4.6	39.4	0.74	20.32
Urb	174	2204.3	2.23	2.23	23	20.8	8	7.4	7.4	176.9	0.58	35.04
Urb	512	50.3	21.5	2.24	49	25.3	33	11.7	11.7	93.7	1.08	72.15
SW (desert)	Agr	2	1.8	36.7	1.84	24	18.6	5	7	-1.2	n.d.	0.13
	Agr	4	3.9	13.6	3.85	2	20.5	13	1	5.0	n.d.	n.d.
	Agr	297	4.4	18.9	0.89	4	16.3	199	5	-14.5	0.28	3.13
	Ref	0	1.5	55.9	0.88	12	18.0	82	12	-0.5	n.d.	0.01
	Ref	4	3.6	2.5	0.96	6	18.0	268	23	-2.9	n.d.	0.14
	Ref	58	2.0	31.8	2.20	21	25.4	92	4	22.5	1.46	1.84
	Urb	13	3.4	50.2	2.39	18	23.3	23	10	-4.6	n.d.	n.d.
	Urb	99	65.2	20.9	n.d.	28	20.0	n.d.	n.d.	n.d.	n.d.	n.d.
	Urb	4	9.8	25.2	1.04	18	22.2	9	6	0.4	n.d.	n.d.
	Urb	50	3.0	2.8	1.97	158	12.0	39	11.4	39.3	n.d.	0.16
WY (dry coniferous forest)	Agr	1	2.9	15.3	0.79	131	16.0	54	7.1	-12.8	n.d.	n.d.
	Agr	28	1.1	4.4	0.69	154	11.2	24	12.0	-7.8	0.04	0.15
	Ref	0	1.7	2.4	2.18	56	16.8	79	4.0	12.2	n.d.	0.004
	Ref	19	3.8	10.0	1.29	65	12.8	79	12.6	-10.1	n.d.	n.d.
	Ref	3	2.2	n.d.	1.56	268	14.3	90	9.8	-21.5	n.d.	n.d.
	Urb	1	1.0	2.1	0.29	110	18.6	36	10.0	17.2	n.d.	0.37
	Urb	152	1.0	3.2	0.39	9	10.9	20	1.5	n.d.	n.d.	n.d.
	Urb	235	4.3	5.9	0.29	103	9.9	19	n.d.	96.5	0.11	1.14

Agr, agricultural; Ave temp, average temperature; DOC, dissolved organic carbon; k<sub>2</sub>, air-water gas exchange rate for oxygen at 20 °C; n.d., no data or below detection limit; N<sub>2</sub>O yield, N<sub>2</sub>O/(N<sub>2</sub>O + N<sub>2</sub>); Ref, reference; SRP, soluble reactive phosphorus; Urb, urban.